

Quantum Asymmetry and Noisy Multimode Interferometry

Francesco Albarelli^{1,2}, Mateusz Mazelanik^{3,1}, Michał Lipka³, Alexander Streltsov³,


Michał Parniak^{3,4} and Rafał Demkowicz-Dobrzański¹

¹*Faculty of Physics, University of Warsaw, 02-093 Warsaw, Poland*

²*Dipartimento di Fisica “Aldo Pontremoli”, Università degli Studi di Milano, via Celoria 16, 20133 Milan, Italy*

³*Centre for Quantum Optical Technologies, Centre of New Technologies, University of Warsaw, 02-097 Warsaw, Poland*

⁴*Niels Bohr Institute, University of Copenhagen, 2100 Copenhagen, Denmark*

 (Received 31 July 2021; revised 13 April 2022; accepted 9 May 2022; published 17 June 2022)

Quantum asymmetry is a physical resource that coincides with the amount of coherence between the eigenspaces of a generator responsible for phase encoding in interferometric experiments. We highlight an apparently counterintuitive behavior that the asymmetry may *increase* as a result of a *decrease* of coherence inside a degenerate subspace. We intuitively explain and illustrate the phenomena by performing a three-mode single-photon interferometric experiment, where one arm carries the signal and two noisy reference arms have fluctuating phases. We show that the source of the observed sensitivity improvement is the reduction of correlations between these fluctuations and comment on the impact of the effect when moving from the single-photon quantum level to the classical regime. Finally, we also establish the analogy of the effect in the case of entanglement resource theory.

DOI: [10.1103/PhysRevLett.128.240504](https://doi.org/10.1103/PhysRevLett.128.240504)

Superposition of quantum states is a fundamental principle of quantum mechanics and the ability to create and preserve coherent superpositions is the essential prerequisite for the realization of all kinds of quantum technologies. In recent years, the basic intuition that quantum superposition is a valuable and fragile resource has been formalized within the mathematical framework of quantum resource theories [1–3]. The mathematical notion of coherence relies on the decomposition of the Hilbert space of the system into subspaces; usually the orthogonal eigenspaces of an observable. This is actually a subcase of the more general resource theory of quantum asymmetry [4,5], where the resource is the degree to which a quantum state breaks a certain symmetry, defined in terms of a Lie group. Quantum asymmetry has been recognized as the relevant physical resource in a variety of operational settings: reference frame alignment [6–8], quantum thermodynamic tasks [9–11], quantum speed limits [12,13], assessing macroscopic quantumness [14–16], and, most importantly for this Letter, quantum metrology [5,17–19]. In this framework, the coherence of a quantum state with respect to the eigenspaces of an observable G corresponds to the asymmetry with respect to the one-parameter group of translations $e^{i\theta G}$; in the following, the term quantum asymmetry will be used to refer to this specific notion.

In this work, we focus on a qutrit example, which is the simplest case where a nontrivial generator G with a degenerate eigenvalue exists. Our main result is to show that the sensitivity to the phase θ , which also quantifies the G asymmetry, is increased for probe states that are more dephased in the degenerate subspace, thus effectively

“noisier,” in a sense that will be made more precise. Furthermore, we also show that a similar, yet less pronounced, behavior appears when the dephasing channel \mathcal{E} is used for entanglement distribution.

We study the phenomena in terms of a physical realization of the system as a three-arm interferometer and we complement our theoretical analysis with a single-photon optical experiment that confirms our predictions.

While quantum coherence theory is intimately related with multiple phase interferometry [20–26], in this Letter we focus on the estimation of a single phase θ , imprinted onto a signal mode, while the phases of the other reference modes fluctuate, generalizing the paradigmatic phase diffusion model [27–33]. Interestingly, this interferometric point of view will shed light on the apparently unintuitive effect observed in the abstract description: we will show that an increased dephasing in the degenerate subspace is caused by less correlated fluctuations of the reference phases, which allows to decrease the measurement noise without altering the signal.

Asymmetry and the quantum Fisher information.—Quantum resource theories, with the entanglement theory as the most famous example [34], arise naturally when a set of quantum states can be regarded as free and any state outside of it as a resource [2]. This immediately defines also free operations, i.e., quantum channels that cannot transform free states into resources. In the resource theory of asymmetry the starting point is the representation of a symmetry group. In particular, we consider a finite-dimensional representation of $U(1)$: $U_\theta = e^{-i\theta G}$, where $G = \sum_k E_k |k\rangle\langle k|$ is the Hermitian generator, $|k\rangle$ are its

eigenstates, and E_k its eigenvalues, which can be degenerate. Resource states \mathcal{G} are those *not* invariant under the action of U_θ and free operations those commuting with U_θ . If G is nondegenerate, \mathcal{G} is the set of incoherent states with no off-diagonal elements in the eigenbasis; otherwise, all superpositions of eigenstates of the same degenerate eigenvalue are also free.

There are inequivalent ways to quantify the asymmetry of a quantum state, called asymmetry monotones, which must not increase under free operations [35]. When U_θ is regarded as a θ parameter encoding operation on a quantum state, the quantum Fisher information (QFI) of the state is an asymmetry monotone [19]. It is defined as $\mathcal{F}_\theta(\rho) = \text{Tr}[\rho_\theta L_\theta^2]$, where $\rho_\theta = U_\theta \rho U_\theta^\dagger$ and the symmetric logarithmic derivative (SLD) operator L_θ is defined as $2(d\rho_\theta/d\theta) = L_\theta \rho_\theta + \rho_\theta L_\theta$. The QFI quantifies the sensitivity of ρ to the imprinted phase θ , since the quantum Cramér-Rao bound (CRB) states that the variance of any unbiased estimator $\tilde{\theta}$ is lower bounded as [36–38] $\Delta^2 \tilde{\theta} \geq [1/\nu \mathcal{F}_\theta(\rho)]$, where ν is the number of repetitions and the bound is saturable for large ν .

Qutrit model.—Consider a three-level system (qutrit) and the generator $G = E_1(|1\rangle\langle 1| + E_2(|2\rangle\langle 2| + |3\rangle\langle 3|)$, where we have fixed an orthonormal basis $\{|2\rangle, |3\rangle\}$ of the degenerate eigenspace, singled out by the dephasing channel \mathcal{E} , which describes a decrease of coherence between the two eigenspaces by a factor η and between $\{|2\rangle, |3\rangle\}$ by a factor κ :

$$\mathcal{E}(\rho) = \begin{bmatrix} \rho_{11} & \eta\rho_{12} & \eta\rho_{13} \\ \eta\rho_{21} & \rho_{22} & \kappa\rho_{23} \\ \eta\rho_{31} & \kappa\rho_{32} & \rho_{33} \end{bmatrix}. \quad (1)$$

The channel is physical (a completely positive map) provided

$$0 \leq \eta \leq 1 \wedge 2\eta^2 - 1 \leq \kappa \leq 1; \quad (2)$$

we restrict to real-valued η and κ without loss of generality.

We consider the phase parameter θ unitarily encoded by G , i.e., $\mathcal{E}_\theta(\rho) = e^{-i\theta G} \mathcal{E}(\rho) e^{i\theta G}$ and to study the effect of dephasing we focus on a pure probe state $\rho_0 = |\psi_0\rangle\langle\psi_0|$ that is a superposition of states from different eigenspaces: $|\psi_0\rangle = \sqrt{q}|1\rangle + \sqrt{[(1-q)/2]}(|2\rangle + |3\rangle)$, with $0 \leq q \leq 1$. The corresponding QFI is

$$\mathcal{F}[\mathcal{E}_\theta(\rho_0)] = \frac{8(E_1 - E_2)^2 \eta^2 (1-q)q}{\kappa + 1 + q(1-\kappa)} \quad (3)$$

and quantifies both the asymmetry of the state $\mathcal{E}(\rho)$ and its phase sensitivity. Details on the calculation are in the Supplemental Material [39].

As expected, the QFI is a monotonically increasing function of η . However, for any value of η and q it is a

decreasing function of κ . This means that more dephasing in the degenerate subspace gives higher sensitivity to the imprinted phase θ , despite the state becoming in some sense noisier—decreasing κ from 1 (no dephasing) to a value $\kappa \geq 0$ always decreases its purity $\text{Tr}\rho^2$. While this result appears counterintuitive, we stress that it does not violate the monotonicity property of the QFI. According to Eq. (2), a channel with $\eta = 1$ and $\kappa < 1$ is not physical. Thus, it is not possible to see the two decoherence effects parametrized by η and κ as the action of separate channels.

Since \mathcal{E} and $e^{-i\theta G}$ commute, the overall channel \mathcal{E}_θ also describes a physical process in which noise and parameter encoding happen simultaneously. While the QFI quantifies the asymmetry of the noisy state $\mathcal{E}(\rho)$, from a quantum metrology point of view, one assumes that the channel \mathcal{E}_θ is given and optimizes the probe state. The so-called channel QFI $\max_\rho \mathcal{F}[\mathcal{E}_\theta(\rho)] = 8\eta^2(\kappa - 2\sqrt{2}\sqrt{\kappa+1} + 3)/(\kappa - 1)^2$ is obtained for $q = q_{\text{opt}} = 1/[\sqrt{2}/(\kappa+1) + 1]$; apart from the $\kappa = 1$ case, the optimal state is not a balanced superposition.

Our results are not due to a peculiar behavior of the QFI; we have also evaluated the relative entropy of asymmetry [7,8,44,45] and observed a qualitatively analogous behavior, with the maximal asymmetry achieved for a slightly different value of q . However, the simplest and in some sense the most intuitive measure, i.e., the sum of the trace norm of the modes of asymmetry [17], does not depend on κ and hence would not reveal the effect.

Interferometric realization.—We now show a simple physical explanation of the apparently counterintuitive result. Consider a three-mode interferometer, as depicted in Fig. 1. A single photon is prepared in a three mode superposition by the action of two beam splitters, creating the initial state $|\psi_0\rangle$. Then the phase θ is imprinted on the first signal mode, while the second and third reference modes do not have stable phases but are subject to random phase fluctuations ϕ_1 and ϕ_2 , with zero mean and a joint probability distribution $P(\phi_1, \phi_2)$. The simplest choice is given by correlated “phase kicks,” i.e., ϕ_1 and ϕ_2 fluctuate to two equal and opposite values $\pm\phi_0 \in [-(\pi/2), (\pi/2)]$ with probabilities $P(\phi_0, \phi_0) = P(-\phi_0, -\phi_0) = \frac{1}{4}(1+c)$ and $P(\phi_0, -\phi_0) = P(-\phi_0, \phi_0) = \frac{1}{4}(1-c)$, where $c = \mathbb{E}[\phi_1\phi_2]/\sqrt{\mathbb{E}[\phi_1^2]\mathbb{E}[\phi_2^2]}$ is the correlation coefficient, ranging from perfectly correlated $c = 1$ to perfectly anticorrelated $c = -1$ and \mathbb{E} denotes the expectation with respect to $P(\phi_1, \phi_2)$. These parameters are related to the previous ones as

$$\begin{aligned} \eta &= \mathbb{E}[e^{i\phi_1}] = \mathbb{E}[e^{i\phi_2}] = \cos\phi_0, \\ \kappa &= \mathbb{E}[e^{i(\phi_1-\phi_2)}] = \cos^2\phi_0(1-c) + c = \eta^2 + c(1-\eta^2), \end{aligned} \quad (4)$$

as the action of the dephasing channel corresponds to $\mathcal{E}(\star) = \mathbb{E}[e^{-i(\phi_2|2\rangle\langle 2| + \phi_3|3\rangle\langle 3|)} \star e^{i(\phi_2|2\rangle\langle 2| + \phi_3|3\rangle\langle 3|)}]$. The parameter ϕ_0 represents the magnitude of the phase kicks

and is directly linked to the parameter η , which we will keep using for convenience. The parameter κ on the other hand, depends both on ϕ_0 and on the correlation coefficient c , and the whole range of physical values of κ in Eq. (2) can be obtained by varying c . It is also possible to obtain the same qutrit channel \mathcal{E} if $P(\phi_1, \phi_2)$ is a bivariate Gaussian distribution, similarly to the standard phase diffusion model in a Mach-Zehnder (MZ) interferometer [27,29,46]. The qualitative picture remains the same: the less correlated (i.e., more anticorrelated) ϕ_1 and ϕ_2 are, the higher the phase sensitivity is. However, for $c < 0$ the effect is less pronounced, since this noise model does not reproduce the full range of physical κ in Eq. (2), as detailed in Sec. B of Ref. [39], where we also present experimental results for this model.

In Fig. 1 we also show the optimal detection scheme that saturates the QFI, formally a projective measurement on the eigenstates of the SLD L_{θ_0} : $(1/\sqrt{2})|1\rangle \pm i(e^{-i\theta_0}/2)(|2\rangle + |3\rangle)$ and $(1/\sqrt{2})(|2\rangle - |3\rangle)$. Here θ_0 is the working point around which we estimate small variations of the parameter. Setting $\theta_0 = 0$ for concreteness, the probabilities of registering the photon at one of the three detectors read

$$\begin{aligned} p_1 &= \frac{1-p_3}{2} + f_\theta, & f_\theta &= v\eta\sqrt{q(1-q)}\sin\theta, \\ p_2 &= \frac{1-p_3}{2} - f_\theta & p_3 &= \frac{1}{2}(1-q)(1-v\kappa), \end{aligned} \quad (5)$$

where we have also introduced an additional visibility parameter $0 \leq v \leq 1$ that takes into account imperfect interference—see Sec. C of Ref. [39] for a complete derivation.

If $v = 1$ and $\kappa = 1$, detector “3” never clicks ($p_3 = 0$). This corresponds to perfectly correlated phases fluctuations, $c = 1$, and results in an effective standard qubit dephasing model (modes 2 and 3 can be regarded as a single mode). When κ is decreased, which corresponds to moving from the perfectly correlated noise ($c = 1$) via uncorrelated ($c = 0$) to the perfectly anticorrelated one

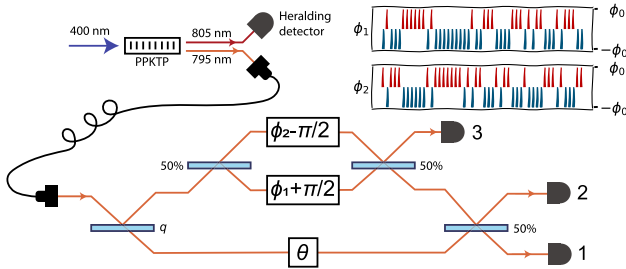


FIG. 1. Schematics of the experimental demonstration of phase estimation in the three-arm interferometer with correlated noise. Heralded single photons from spontaneous parametric down-conversion are used to probe the system with noisy phases ϕ_1 and ϕ_2 to estimate the phase θ . Inset shows an example realization of phase noise with high anticorrelation.

($c = -1$), detector 3 filters out the “anticorrelated” part of the phase noise. Doing so, it effectively increases the visibility of the interference pattern observed in detectors “1” and “2” [note that the θ dependent “fringe terms” f_θ in p_1 and p_2 do not depend on κ , see Eq. (5)]:

$$\mathcal{V} = \frac{p(1|\frac{\pi}{2}) - p(1|\frac{-\pi}{2})}{p(1|\frac{\pi}{2}) + p(1|\frac{-\pi}{2})} = \frac{4v\eta\sqrt{q(1-q)}}{1+q+v\kappa(1-q)} \quad (6)$$

and leads to a better phase sensitivity. The possibility of filtering out the anticorrelated part of the noise is the essence of the counterintuitive behavior of the QFI.

Experimental results.—We have realized the proposed model in a photonic experiment that is schematically depicted in Fig. 1. The two reference arms of the three-arm interferometer are piezoactuated, which allow us to control both the phase to be measured θ and the zero-mean fluctuations ϕ_1 and ϕ_2 , (see Sec. D of the Supplemental Material [39] for a detailed description of the physical implementation). The interferometer outputs are coupled to single mode fibers connected to superconducting nanowire single photon detectors (SNSPD) with coincidence counters. We feed the interferometer with heralded single photons at 795 nm generated in a continuously driven nondegenerate (795 and 805 nm) SPDC source. We run the experiment in 80-sec-long intervals and accumulate coincidences for various parameter settings $\{\theta, \phi_0, c\} \in [0, 2\pi] \times [0, 1.16] \times [-1, 1]$. To emulate the discrete $\pm\phi_0$ phase kicks we measure each $\{\phi_1, \phi_2\}$ subsetting separately and combine the results according to the given c . The compact form of the interferometer provides sufficient 15-min-long phase stability. To maintain long-time stability, each measurement interval is preceded by a calibration step consisting of scanning the actuators and observing intensity fringes (without heralding) at the interferometer outputs. The calibration step not only allows us to stabilize θ value but also provides information about the intrinsic visibility $v \approx 0.97$ and relative efficiencies χ in the three measurement ports $\chi(p_2/p_1) \approx 0.95$, $\chi(p_3/p_1) \approx 1.61$. We first compare the measured coincidence distributions with the theoretical predictions given by Eq. (5). To recover the probabilities from measured counts we normalize the number of detected photons accounting for different net efficiencies at the interferometer output ports. In Figs. 2(a)–2(d) we show examples of normalized counts \tilde{N} measured for a range of θ phases along with the expected curves corresponding to the same η and c parameters. From those we recover the visibilities that are shown on a common plot in Fig. 2(e). The solid lines represent the expected behavior as described by Eq. (6).

In order to validate the improvement of the phase estimation precision in the presence of increasingly anticorrelated noise, we have implemented an estimation procedure based on the efficient locally unbiased estimator (at the working point $\theta_0 = 0$):

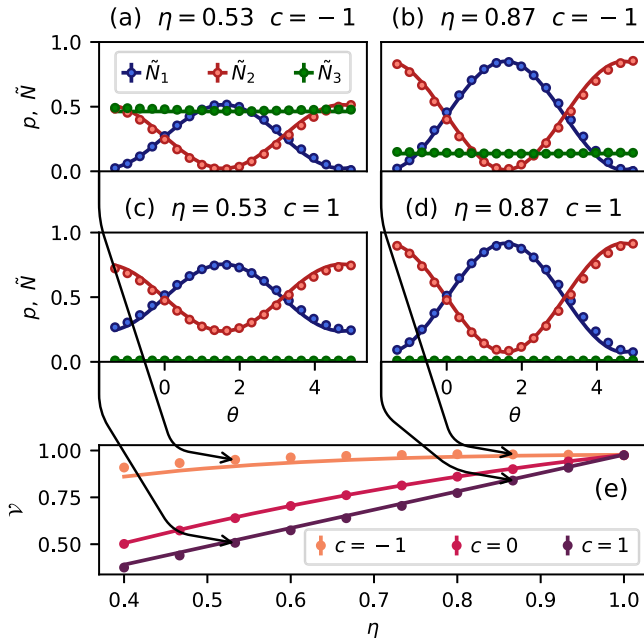


FIG. 2. (a)–(d) Exemplary probability distributions for two different η settings in the perfectly correlated and anticorrelated case. The points correspond to measured and renormalized coincidences (\tilde{N}). (e) Measured (points) and expected (solid lines) visibility parameter for chosen η and c parameters.

$$\hat{\theta} = \frac{N_1 - N_2}{2v\eta\sqrt{(1-q)q(N_1 + N_2 + N_3)}}, \quad (7)$$

where N_i denotes the detected photon counts in the given output port. We evaluate the estimator on 10^4 randomly prepared sets of measurement outcomes each containing 10^5 samples in total. Each set is prepared by randomly sampling (with repetitions) from the 10^5 measured single-photon counts at the $\theta_0 = 0$ point. The resulting single-photon estimation precision, defined as the inverse of the estimator variance divided by the total number of detected photons, is presented in Fig. 3. The error bars correspond to chi-squared 99% confidence interval. The rescaling to single-photon value allows us to compare the achieved precision with the classical FI (solid lines), calculated for the model probabilities [Eq. (5)] that take into account the finite interference visibility v . The dashed lines represent the ultimate bound given by the QFI. In Fig. 3 we clearly see that the estimation precision improves for the anticorrelated noise as predicted by the FI and QFI.

Entanglement.—A similar effect can also be observed for entanglement. Let us apply the channel \mathcal{E} to one part of the entangled state $|\psi\rangle^{AB} = \sqrt{q}|11\rangle + \sqrt{[(1-q)/2]}(|22\rangle + |33\rangle)$. The resulting state takes the form of a maximally correlated state [47]:

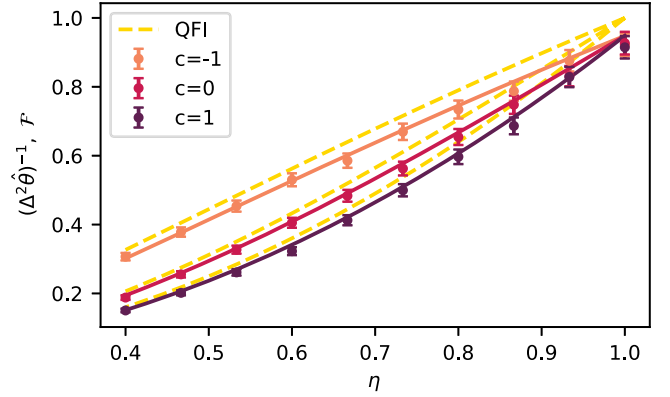


FIG. 3. Precision of θ estimation (points) for set of η and c parameters compared with CRB and QCRB given by FI (solid lines) and QFI, respectively.

$$\rho^{AB} = \mathbb{1} \otimes \mathcal{E}(|\psi\rangle\langle\psi|^{AB}) = \sum_{i,j} \alpha_{ij} |ii\rangle\langle jj| \quad (8)$$

with parameters $\alpha_{11} = q$, $\alpha_{22} = \alpha_{33} = (1-q)/2$, $\alpha_{12} = \alpha_{21} = \alpha_{13} = \alpha_{31} = \eta\sqrt{q(1-q)}/2$, and $\alpha_{23} = \alpha_{32} = \kappa(1-q)/2$. In fact, these states can be regarded as the maximally correlated states associated to the qutrit states in Eq. (1). It is known that coherence properties of a quantum state are closely related to entanglement properties of the corresponding maximally correlated state [1,48]. Following this analogy, it is reasonable to expect that the results presented above will also extend to entanglement of the states in Eq. (8). For this, we investigate distillable entanglement of ρ^{AB} , characterizing how many singlets can be extracted from the state ρ^{AB} via local operations and classical communication in the asymptotic limit [49,50]. While the distillable entanglement is hard to evaluate in general, a closed expression exists for states of the form (8): $E_d(\rho^{AB}) = S(\rho^B) - S(\rho^{AB})$ with the von Neumann entropy $S(\rho) = -\text{Tr}(\rho \log_2 \rho)$. For this class of states only the global entropy $S(\rho)$ depends on κ and the distillable entanglement $E_d(\rho^{AB})$ is equal to the relative entropy of coherence of the state in Eq. (1) with respect to the orthonormal basis $\{|1\rangle, |2\rangle, |3\rangle\}$ [1,48]. We can intuitively think that there are two competing effects at play: reducing κ decreases the coherence in the subspace spanned by $|2\rangle$ and $|3\rangle$, but at the same time increases coherence between this subspace and $|1\rangle$. For this reason, the effect is far less pronounced than with the QFI, but there is still a region of parameters where the entanglement increases when moving from a positive value of κ to a smaller (yet positive) value. More details on the entanglement analysis are presented in Sec. F of Ref. [39].

Classical light.—It is natural to wonder what would happen if instead of a single photon we used classical light, i.e., a coherent input state $|\alpha\rangle$. In this case we use a Gaussian phase fluctuation model $P(\phi_1, \phi_2)$, see details in Sec. B of Ref. [39]. We consider an estimation strategy,

analogous to the standard MZ interferometer, based on the photon number difference $I^- = n_1 - n_2$, optimal in the single-photon regime, and we evaluate the variance using error propagation: $\Delta^2\theta = \Delta^2I^- / [(d/d\theta)E[|I^-|]]^2$, where the Δ^2I^- includes also the contribution of the distribution $P(\phi_1, \phi_2)$ of the fluctuating reference phases. In Sec. D of Ref. [39] we show that

$$\Delta^2\theta = \frac{1}{|\alpha|^2 \mathcal{F}_\theta} + \frac{1}{2}(\eta^{-2} - \eta^2 + \eta^{-2c} - \eta^{2c}), \quad (9)$$

where the first terms contains the single-photon QFI (3) [with the η and κ now related to the parameters σ and c of the Gaussian noise model, see Eq. (B2) in the Supplemental Material [39]]. This result implies that this strategy with classical light performs worse than repeating a single photon experiment many times, but for a weak coherent state we have the same sensitivity per average photon, i.e., $(|\alpha|^2 \Delta^2\theta)^{-1} \xrightarrow{\alpha \rightarrow 0} \mathcal{F}_\theta$. For an intense beam the variance saturates to a constant value, as in standard phase diffusion [29,31], and only vanishes for $c = -1$.

Finally, we can also consider a “naive classical” strategy, without any interference between the two reference modes, which is equivalent to two separate MZ interferometers sensing the phase shifts $\theta - \phi_1$ and $\theta - \phi_2$. In this case one finds the same structure as in Eq. (9), but the first term corresponds to the QFI evaluated at $c = 1$, i.e., it does not improve by reducing the correlations. Details are given in Sec. G.2 of Ref. [39].

Discussion.— Starting with an abstract model of the loss of coherence within a degenerate subspace of the generator of a phase shift, we have discussed and demonstrated the nonintuitive effect of an increased sensing precision. By considering the optimal interferometric scheme we have related such an improvement to the possibility of filtering out the anticorrelated part of the dephasing noise. This effect may be of practical importance in interferometric schemes where one is able to cause the phase fluctuations affecting multiple reference modes to become uncorrelated (by, e.g., separating them spatially) or even make them anticorrelated (if thermal fluctuations were responsible for dephasing, while the materials had opposite thermal and temperature coefficient of the refractive index). Interestingly, the most significant gains from the effect can be obtained at the single photon level, and when the light from both the reference arms is interfered with each other before eventually interfering with the light from the signal arm. The results can be generalized to obtain qualitatively similar effects in the case of d reference modes instead of just two.

We thank Konrad Banaszek, Wojtek Górecki, and Wojciech Wasilewski for fruitful discussions. F.A. and R.D.D. were supported by National Science Center (Poland) Grant No. 2016/22/E/ST2/00559. R.D.D. was

additionally supported by National Science Center (Poland) Grant No. 2020/37/B/ST2/02134.. M. M., M. L., A. S., and M. P. are supported by the Foundation for Polish Science “Quantum Optical Technologies” project (MAB/2018/4), carried out within the International Research Agendas programme of the Foundation for Polish Science co-financed by the European Union under the European Regional Development Fund.

- [1] A. Streltsov, G. Adesso, and M.B. Plenio, Colloquium: Quantum coherence as a resource, *Rev. Mod. Phys.* **89**, 041003 (2017).
- [2] E. Chitambar and G. Gour, Quantum resource theories, *Rev. Mod. Phys.* **91**, 025001 (2019).
- [3] K.-D. Wu, A. Streltsov, B. Regula, G.-Y. Xiang, C.-F. Li, and G.-C. Guo, Experimental progress on quantum coherence: Detection, quantification, and manipulation, *Adv. Quantum Technol.* **4**, 2100040 (2021).
- [4] G. Gour and R.W. Spekkens, The resource theory of quantum reference frames: Manipulations and monotones, *New J. Phys.* **10**, 033023 (2008).
- [5] I. Marvian and R. W. Spekkens, How to quantify coherence: Distinguishing speakable and unspeakable notions, *Phys. Rev. A* **94**, 052324 (2016).
- [6] S. D. Bartlett, T. Rudolph, and R. W. Spekkens, Reference frames, superselection rules, and quantum information, *Rev. Mod. Phys.* **79**, 555 (2007).
- [7] J. A. Vaccaro, F. Anselmi, H. M. Wiseman, and K. Jacobs, Tradeoff between extractable mechanical work, accessible entanglement, and ability to act as a reference system, under arbitrary superselection rules, *Phys. Rev. A* **77**, 032114 (2008).
- [8] G. Gour, I. Marvian, and R. W. Spekkens, Measuring the quality of a quantum reference frame: The relative entropy of frameness, *Phys. Rev. A* **80**, 012307 (2009).
- [9] M. Lostaglio, D. Jennings, and T. Rudolph, Description of quantum coherence in thermodynamic processes requires constraints beyond free energy, *Nat. Commun.* **6**, 6383 (2015).
- [10] M. Lostaglio, K. Korzekwa, D. Jennings, and T. Rudolph, Quantum Coherence, Time-Translation Symmetry, and Thermodynamics, *Phys. Rev. X* **5**, 021001 (2015).
- [11] K. Korzekwa, M. Lostaglio, J. Oppenheim, and D. Jennings, The extraction of work from quantum coherence, *New J. Phys.* **18**, 023045 (2016).
- [12] I. Marvian, R. W. Spekkens, and P. Zanardi, Quantum speed limits, coherence, and asymmetry, *Phys. Rev. A* **93**, 052331 (2016).
- [13] D. Mondal, C. Datta, and S. Sazim, Quantum coherence sets the quantum speed limit for mixed states, *Phys. Lett. A* **380**, 689 (2016).
- [14] B. Yadin and V. Vedral, General framework for quantum macroscopicity in terms of coherence, *Phys. Rev. A* **93**, 022122 (2016).
- [15] H. Kwon, C.-Y. Park, K. C. Tan, D. Ahn, and H. Jeong, Coherence, asymmetry, and quantum macroscopicity, *Phys. Rev. A* **97**, 012326 (2018).

- [16] F. Fröwis, P. Sekatski, W. Dür, N. Gisin, and N. Sangouard, Macroscopic quantum states: Measures, fragility, and implementations, *Rev. Mod. Phys.* **90**, 025004 (2018).
- [17] I. Marvian and R. W. Spekkens, Modes of asymmetry: The application of harmonic analysis to symmetric quantum dynamics and quantum reference frames, *Phys. Rev. A* **90**, 062110 (2014).
- [18] I. Marvian and R. W. Spekkens, Extending Noether's theorem by quantifying the asymmetry of quantum states, *Nat. Commun.* **5**, 3821 (2014).
- [19] C. Zhang, B. Yadin, Z.-B. Hou, H. Cao, B.-H. Liu, Y.-F. Huang, R. Maity, V. Vedral, C.-F. Li, G.-C. Guo, and D. Girolami, Detecting metrologically useful asymmetry and entanglement by a few local measurements, *Phys. Rev. A* **96**, 042327 (2017).
- [20] S. Dürr, Quantitative wave-particle duality in multibeam interferometers, *Phys. Rev. A* **64**, 042113 (2001).
- [21] B.-G. Englert, D. Kaszlikowski, L. C. Kwek, and W. H. Chee, Wave-particle duality in multi-path interferometers: General concepts and three-path interferometers, *Int. J. Quantum. Inform.* **06**, 129 (2008).
- [22] P. C. Humphreys, M. Barbieri, A. Datta, and I. A. Walmsley, Quantum Enhanced Multiple Phase Estimation, *Phys. Rev. Lett.* **111**, 070403 (2013).
- [23] M. N. Bera, T. Qureshi, M. A. Siddiqui, and A. K. Pati, Duality of quantum coherence and path distinguishability, *Phys. Rev. A* **92**, 012118 (2015).
- [24] E. Bagan, J. A. Bergou, S. S. Cottrell, and M. Hillery, Relations Between Coherence and Path Information, *Phys. Rev. Lett.* **116**, 160406 (2016).
- [25] T. Biswas, M. García Díaz, and A. Winter, Interferometric visibility and coherence, *Proc. R. Soc. Math. Phys. Eng. Sci.* **473**, 20170170 (2017).
- [26] M. Masini, T. Theurer, and M. B. Plenio, Coherence of operations and interferometry, *Phys. Rev. A* **103**, 042426 (2021).
- [27] M. G. Genoni, S. Olivares, and M. G. A. Paris, Optical Phase Estimation in the Presence of Phase Diffusion, *Phys. Rev. Lett.* **106**, 153603 (2011).
- [28] M. G. Genoni, S. Olivares, D. Brivio, S. Cialdi, D. Cipriani, A. Santamato, S. Vezzoli, and M. G. A. Paris, Optical interferometry in the presence of large phase diffusion, *Phys. Rev. A* **85**, 043817 (2012).
- [29] B. M. Escher, L. Davidovich, N. Zagury, and R. L. De Matos Filho, Quantum Metrological Limits via a Variational Approach, *Phys. Rev. Lett.* **109**, 190404 (2012).
- [30] M. D. Vidrighin, G. Donati, M. G. Genoni, X.-M. Jin, W. S. Kolthammer, M. S. Kim, A. Datta, M. Barbieri, and I. A. Walmsley, Joint estimation of phase and phase diffusion for quantum metrology, *Nat. Commun.* **5**, 3532 (2014).
- [31] K. Macieszczak, M. Fraas, and R. Demkowicz-Dobrzański, Bayesian quantum frequency estimation in presence of collective dephasing, *New J. Phys.* **16**, 113002 (2014).
- [32] R. Demkowicz-Dobrzański, M. Jarzyna, and J. Kołodyński, Quantum limits in optical interferometry, in *Progress in Optics, Volume 60*, edited by E. Wolf (Elsevier, Amsterdam, 2015), pp. 345–435.
- [33] H. Scott, D. Branford, N. Westerberg, J. Leach, and E. M. Gauger, Noise limits on two-photon interferometric sensing, *Phys. Rev. A* **104**, 053704 (2021).
- [34] R. Horodecki, P. Horodecki, M. Horodecki, and K. Horodecki, Quantum entanglement, *Rev. Mod. Phys.* **81**, 865 (2009).
- [35] More precise definitions can be found elsewhere [1,2] and are not needed for our discussion.
- [36] C. W. Helstrom, *Quantum Detection and Estimation Theory* (Academic Press, New York, 1976).
- [37] A. S. Holevo, *Probabilistic and Statistical Aspects of Quantum Theory*, 2nd ed. (Edizioni della Normale, Pisa, 2011).
- [38] M. G. A. Paris, Quantum estimation for quantum technology, *Int. J. Quantum. Inform.* **07**, 125 (2009).
- [39] See Supplemental Material at <http://link.aps.org/supplemental/10.1103/PhysRevLett.128.240504>, which includes Refs. [40–43].
- [40] V. Vedral, M. B. Plenio, M. A. Rippin, and P. L. Knight, Quantifying Entanglement, *Phys. Rev. Lett.* **78**, 2275 (1997).
- [41] E. Rains, A semidefinite program for distillable entanglement, *IEEE Trans. Inf. Theory* **47**, 2921 (2001).
- [42] Y. Zinchenko, S. Friedland, and G. Gour, Numerical estimation of the relative entropy of entanglement, *Phys. Rev. A* **82**, 052336 (2010).
- [43] M. W. Girard, Y. Zinchenko, S. Friedland, and G. Gour, Erratum: Numerical estimation of the relative entropy of entanglement [*Phys. Rev. A* **82**, 052336 (2010)]; *Phys. Rev. A* **91**, 029901(E) (2015).
- [44] J. Åberg, Quantifying superposition, [arXiv:quant-ph/0612146](https://arxiv.org/abs/quant-ph/0612146).
- [45] M. J. W. Hall and H. M. Wiseman, Does Nonlinear Metrology Offer Improved Resolution? Answers from Quantum Information Theory, *Phys. Rev. X* **2**, 041006 (2012).
- [46] M. Szczykulska, T. Baumgratz, and A. Datta, Reaching for the quantum limits in the simultaneous estimation of phase and phase diffusion, *Quantum Sci. Technol.* **2**, 044004 (2017).
- [47] E. M. Rains, Bound on distillable entanglement, *Phys. Rev. A* **60**, 179 (1999).
- [48] A. Winter and D. Yang, Operational Resource Theory of Coherence, *Phys. Rev. Lett.* **116**, 120404 (2016).
- [49] C. H. Bennett, G. Brassard, S. Popescu, B. Schumacher, J. A. Smolin, and W. K. Wootters, Purification of Noisy Entanglement and Faithful Teleportation via Noisy Channels, *Phys. Rev. Lett.* **76**, 722 (1996).
- [50] M. B. Plenio and S. Virmani, An introduction to entanglement measures, *Quantum Inf. Comput.* **7**, 1 (2007).